Journal of Catalysis **190,** 276–283 (2000)
doi:10.1006/jcat.1999.2748, available online at http://www.idealibrary.com on IDEAL®

Selective Dehydroaromatization of Methane toward Benzene on Re/HZSM-5 Catalysts and Effects of CO/CO_2 Addition

Linsheng Wang,[1] Ryuichiro Ohnishi, and Masaru Ichikawa[2]

Catalysis Research Center, Hakkaido University, Kita-Ku, N-11, W-10, Sapporo 060, Japan

Received July 8, 1999; revised October 25, 1999; accepted November 1, 1999

The novel rhenium catalyst Re/HZSM-5 was studied for the catalytic performance of methane dehydrocondensation at 3 atm and 873–1023 K. It was found that C_2 hydrocarbons and aromatic compounds such as benzene and naphthalene were catalytically obtained with a considerable evolution of hydrogen. High methane conversion (8–12%) and rates of benzene formation obtained on the Re/HZSM-5 catalyst were similar, under the experimental conditions used, to that on Mo/HZSM-5, which has been thought to be a unique catalyst for the reaction. In contrast to the molybdenum carbide (Mo_2C) as the active phase for the reaction on Mo/HZSM-5, EXAFS and TG/DTA/mass studies suggest that the metallic Re on HZSM-5 is responsible for the catalytic dehydrocondensation of methane toward C_2 hydrocarbons, benzene, and naphthalene. High and stable conversion of methane and high selectivities (70–87% based on carbon) of C_2 hydrocarbons and benzene have been attained in the catalytic dehydrocondensation of methane on Re/HZSM-5 with CO/CO_2 added in methane feed.

Key Words: **dehydrocondensation; methane with CO/CO_2; Re/HZSM-5; benzene.**

1. INTRODUCTION

In recent years the catalytic dehydrocondensation of methane to yield bulky hydrogen and useful petrochemical feedstocks such as ethene and benzene has been a challenging and intriguing approach in heterogeneous catalysis. Since the first report on the nonoxidative conversion of methane to benzene on Mo/HZSM-5 in 1993 (1), there have been many works regarding the catalyst characterization by XRD (2, 3, 22), XPS (4, 6–8, 13), Si/Al-NMR (10, 22), and XAFS (15, 16, 20), its mechanism, and the bifunctional roles of Mo carbide and HZSM-5 in the methane conversion to benzene on Mo/HZSM-5 (5, 7–9, 22). Nevertheless, it is a vital drawback for the industrial technology that the activities of the Mo/HZSM-5 in the methane conversion decline abruptly in a few hours due to the serious coke formation. To solve this issue, we first reported (14, 15, 17) that adding of a few percent of CO/CO_2 to methane feed results in an effective improvement of their catalyst stability for more than 100 h owing to the substantial removal of coke with CO/CO_2 on Mo/HZSM-5 and Mo–Co(Fe)/HZSM-5. As another approach, many transition metal ions such as Mo, W, Fe, V, Cu, Zn, and Cr were tested to activate methane (8, 10, 19). However, it was found that Mo/HZSM-5 is still the most promising catalytic system for the methane aromatization reaction above 923 K. Further, there are controversial problems about the reasonable mechanism and the active phase of metals (carbide for Mo and oxides for Fe, V, Cr, W, and Zn) (12, 18) for the methane dehydroaromatization. This paper will present the new, novel, and promising system of Re/HZSM-5 for the catalytic dehydrocondensation of methane to yield benzene and ethene at 3 atm and 873–1023 K. We will discuss the active phase of Re/HZSM-5 responsible for the methane activation, compared with that of Mo carbide. The HZSM-5-supported rhenium catalysts have been characterized by EXAFS and TG/DTA/mass studies. Further, the mechanism of catalytic dehydrocondensation of methane on Re/HZSM-5 was discussed in conjunction with the role of CO/CO_2 addition to methane feed to effectively reduce the coke formation and improve their catalyst stability.

2. EXPERIMENTAL PROCEDURES

2.1. *Materials and Catalyst Preparation*

Re/HZSM-5 catalysts, at 10 wt% loading, were prepared by impregnation (incipient wetness) of NH_4ZSM-5 ($SiO_2/Al_2O_3 = 40$; surface area, 925 m^2/g; Tosoh Co.) with the aqueous solution of $(NH_4)_2ReO_4 \cdot 4H_2O$. The resulting materials were dried at 393 K and calcined in air at 773 K for 4 h, as reported in the previous literatures for the Mo/HZSM-5 catalysts (11, 14–17). The loading amount of Re on HZSM-5 was quantitatively measured to be 5 wt% by the ICP-analytic method for the solution samples prepared by dissolving in a minimum amount of hydrofluoric acid. The 5 wt% loaded Re/HZSM-5 was designated

---

[1] On leave from Dalian Institute of Chemical Physics, Chinese Academy of Sciences.

[2] To whom correspondence should be addressed.

0021-9517/00 $35.00

5Re/HZSM-5. Excess Re was considered to be lost during calcination.

2.2. *Catalytic Measurement and Kinetic Analysis*

The catalytic tests were carried out under 3 atm of methane with or without CO/CO_2 in a continuous flow system with a quartz reactor of 8 mm i.d. charged with 0.15–0.30 g of catalyst pellets of 20–42 mesh, as has been reported previously (14–17). The feed gas mixture (99.9% pure, Sumitomo Seika Chem. Co.) of 90% CH_4 and 10% Ar was introduced into the reactor at 7.5–100 ml/min [space velocity of methane = 1440–10,000 ml/g cat/h] through a mass flow controller (SEC 400Mk3) after flashing with He at 973 K for 40 min. Hydrocarbon products including C_2–C_4 alkanes (and/or alkenes) and condensable C_6–C_{12} aromatics such as benzene, toluene, xylene, naphthalene, and methylnaphthalene were analyzed by on-line FID gas chromatography on a Porapak-P column using a six-way sampling valve heated to 533 K and the on-line TCD GC for H_2, Ar, CO, CH_4, and CO_2 on an activated carbon column. Condensable materials such as benzene, toluene, xylene, naphthalene, methylnaphthalene, and anthracene were identified by using an off-line GC-mass (Perkin–Elmer, Auto System GC with 910 Q-mass). Using an internal standard analyzing method of 10% v/v Ar in the feed gas of methane with or without CO/CO_2, the conversion of methane, selectivities of hydrocarbon products, and amount of coke formed on the catalysts were evaluated according to the mass balance for carbon. Formation rates of hydrocarbon products and coke formed were calculated as well and were expressed in carbon base.

2.3. *TG/DTA/Mass Experiment*

Temperature-programmed reaction (TPR) was performed using a TG/DTA/mass system (Mac Science Co., TG-DTA2020S) under a methane ($+H_2$, $+CO$)/He stream. Flow rates of the feed gas were 15, 1.8, 5, and 150 ml/min for CH_4, CO, H_2, and He, respectively. Powdered Re/HZSM-5 catalyst (40–50 mg) was mounted in a fused alumina boat, and the evolved products such as H_2, H_2O, CO, CO_2, C_2H_4, C_2H_6, C_6H_6, and $C_{10}H_8$ were continuously monitored with a Thermolab mass spectrometer (VG analysis) at $m/e = 2$, 18, 28, 44, 26, 30, 78, and 128, respectively. The reaction temperature was raised from room temperature to 973 K with a ramping rate of 10 K/min and held there for 30 min. Before the reaction started, the catalyst was heated in a He stream at 873 K for 30 min and, in some cases, was further pretreated with H_2 or methane at 573 or 973 K for 30 min. Temperature-programmed oxidation (TPO) of used catalyst was carried out using the TG/DTA/mass system in a flow of O_2 (20 ml/min) and He (150 ml/min) mixture gas.

2.4. *EXAFS Measurement and Analysis*

The powdered and disk samples were charged under N_2 in an *in situ* EXAFS cell with a KAPTON film window (500 μm) to prevent exposure of the sample to air. Re L_{III}-edge XAFS (X-ray absorption fine structure) measurements were conducted on the samples of Re/HZSM-5 after calcination at 773 K, reduction with hydrogen at 573 K, and reaction with methane at 973 K. The energy and the current of the electron (or positron) were 2.5 GeV and 250 mA and a Si(311) channel cut monochromator was used at Beam Line-10B at the Photon Factory of the National Laboratory for High Energy Physics (KEK-PF; Tsukuba, Japan). EXAFS (extended X-ray absorption fine structure) spectra were analyzed by a computer program supplied by Technos Co. Ltd. (15, 16). The k^3-weighted EXAFS function was Fourier transformed into R space using the k range from 4.6 to 16.3 $Å^{-1}$. The Hanning function used was $\delta = 0.5$ $Å^{-1}$. The phase shift was not corrected for the preliminary Fourier transformation. The fitting EXAFS of the samples in R sphere from 1.98 to 2.98 Å determined the parameters of coordination number (CN), interatomic distance (R), Debye–Waller-like factor (σ), and shift of threshold energy (ΔE_o) to minimize the correction factor. The back-scattering amplitude and phase shift function of Re–Re bonding are corrected using a reference sample of Re powder.

3. RESULTS AND DISCUSSION

3.1. *Catalytic Dehydrocondensation of Methane on Re/HZSM-5*

The conversion of methane was conducted by flowing methane (3 atm) on the 5Re/HZSM-5 catalyst which was charged in the fixed-bed of the quartz reactor. As the catalyst pretreatment, the freshly calcined Re/HZSM-5 was reduced with H_2 at 523 K for 0.5 h before the catalyst was subjected to a methane stream at 973 K. The results are shown in Fig. 1. It was found that C_2 hydrocarbons and aromatic compounds such as benzene and naphthalene were continuously obtained with a considerable evolution of hydrogen (H_2/benzene = 10–25 mol/mol). Further, the careful examination of catalytic performance at the early stage of reaction shows that the formation selectivity of naphthalene was lower and that of benzene was higher on Re/HZSM-5 than that on Mo/HZSM-5 [compare Fig. 1 with Fig. 1 of (22), Fig. 3 of (7), and Fig. 2 of (15)]. The higher activity of hydrogenolysis and molecular shape selectivity were due to the limited size of micropores of HZSM-5 support (5.5 Å) being accessible only to benzene and toluene. The catalytic performances on Re-loaded HZSM-5 were compared at 973 K and at time on stream of 2 and 6 h with that on Mo/HZSM-5 in the literature (14–17, 7, 12, 22), as shown in Table 1. It is of interest to find that, under the reaction

TABLE 1

Comparison of Catalytic Performance on Re- and Mo/HZSM-5-Based Catalysts in Methane Dehydrocondensation[a]

Catalyst	GHSV (h^{-1})	Time (h)	Conv.[b] (%)	Selectivity for product/%[c] C$_2$'s	Bz	Naph	Coke	Reference
5% Re	720	2(6)	7(6)	4(6)	48(56)	11(10)	33(23)	This work
3% Mo	720	2(6)	9(7)	3(5)	41(45)	20(15)	33(32)	Our work (14, 15)
2% MoO$_3$	720	1	6	4	50	NA	43	7
2% Mo	800	2(6)	9(5)	3(4)	57(62)	15(9)	15(15)	12
4% Mo	750	2(6)	10(8)	2(5)	65(69)	18(9)	3(1)	22

[a] Experimental conditions: reaction pressure was 1 atm (except for Re of 3 atm), reaction temperature was 973 K (except for 4% Mo of 950 K), space velocity was calculated assuming packed density of 0.5 g cat/cm^3.

[b] Methane conversion.

[c] C$_2$'s = ethene + ethane, Bz = benzene, Naph = naphthalene, NA = not available.

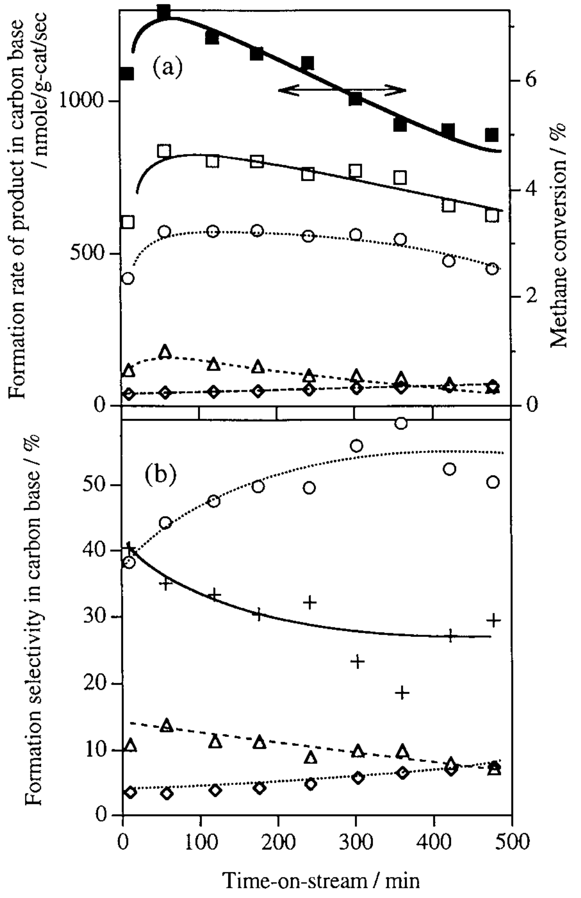

FIG. 1. Catalytic performances of 5Re/HZSM-5 in the dehydrocondensation of methane at 973 K, 3 atm, and 1440 ml/g cat/h of methane space velocity; (a) rates of product formation and of methane conversion and (b) formation selectivities in the methane consumed vs time on steam, where ■ refers to both the methane conversion rate and methane conversion percent. Symbols □, ◇, ○, △, and + refer to the formation rate of product and the formation selectivity of hydrocarbons, ethane + ethene, benzene, naphthalene, and coke, respectively.

conditions examined, the dehydrocondensation of methane on the Re/HZSM-5 catalysts proceeds at rates of product formation comparable to the reference data on Mo/HZSM-5, which has been thought to be a unique catalyst for the methane dehydrocondenzation reaction. Our present results on the Re/HZSM-5 catalyst in the methane dehydrocondensation show that the benzene selectivities based on the consumed methane exceed 65% at the maximum value, due to the modest formation of coke (around 30% selectivity) and polycondensed byproducts.

3.2. Effects of Methane Space Velocity

Figure 2 shows the dependency of methane conversion and rate of benzene formation in the methane conversion on 5Re/HZSM-5 at 1023 K and 3 atm by varying the space velocity of methane from 1440 to 10,000 ml/g cat/h. By increasing the flow rates of methane referred to as the methane space velocity from 1440 to 5000 ml/g cat/h, the initial rate of benzene formation (nmol/s/g cat) is remarkably enhanced by ca. 4 times as shown in Fig. 2a. The initial methane conversion was kept unchanged at 10–10.5% by increasing the methane space velocity from 1440 to 5000 ml/g cat/h as seen in Fig. 2b. These results suggest that the methane conversion to benzene is thermodynamically controlled at the initial stage of the reaction. However, the rate of benzene formation and methane conversion declined drastically as the methane space velocity was higher than 3500 ml/g cat/h. No increase in the initial rate of benzene formation and methane conversion was observed at 10,000 ml/g cat/h of the methane space velocity.

3.3. Active Phase of Re/HZSM-5 Catalysts Responsible for Methane Aromatization by TG/DTA/Mass Studies

The TPR with methane was conducted on 5Re/HZSM-5 using TG/DTA/mass by flowing 10% methane diluted with He while heating from 300 to 973 K. As shown in Fig. 3b, the

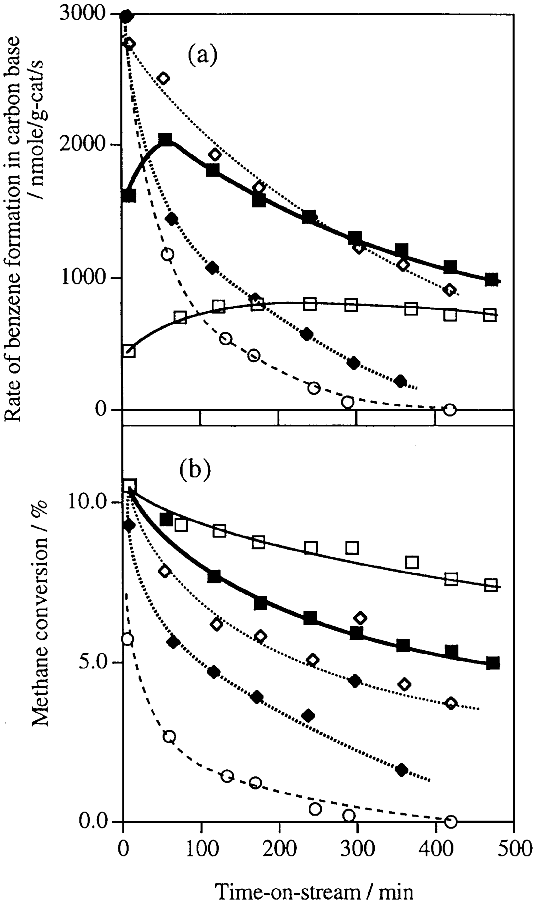

FIG. 2. Catalytic performance of 5Re/HZSM-5 for methane dehydroaromatization with varying methane space velocity at 1023 K and 3 atm; (a) rate of benzene formation and (b) methane conversion: □, ■, ◇, ◆, and ○ for 1440, 2500, 3500, 5000, and 10,000 ml/g cat/h, respectively.

evolution of CO ((**2**), $m/e = 28$), CO_2 ((**3**), $m/e = 44$), and H_2 ((**1**), $m/e = 2$) was observed at 895 K, where the Re oxide impregnated on HZSM-5 was reduced and converted to the active phase by producing a mixture of CO, CO_2, and H_2O. This initiates the dehydrocondensation of methane above 900 K to C_2 hydrocarbons (ethene ((**4**), $m/e = 26$) + ethane ($m/e = 30$)), benzene ((**5**), $m/e = 78$), and naphthalene ((**6**), $m/e = 128$), accompanied with the evolution of hydrogen ((**1**), $m/e = 2$). The DTA pattern (Fig. 3a) in methane reaction on the Re/HZSM-5 shows a considerable endothermic peak at 895 K due to the reaction of Re oxide with methane. The TG pattern in methane flow (Fig. 3a) offers a sharp weight loss at the temperature, being followed with a gradual weight increase possibly due to the carbon accumulation on the Re/HZSM-5 in the methane conversion at 973 K. On the other hand, the reduction of the calcined Re/HZSM-5 occurs at the lower temperature of 850 K with $CH_4 + 1.8\%$ CO flow by the endothermic reaction, evolving CO_2 (**3**) and H_2 (**1**) with the weight loss as shown in Fig. 4a and b. As soon as the reduction subsided, hydrocarbons were formed at lower temperature, 870 K. Further, the reduction of Re-oxide/HZSM-5 occurs at a much lower temperature, around 595 K, with a $CH_4 + 10\%$ H_2 flow by the exothermic reaction, accompanied with the weight loss (not shown). In fact, the methane aromatization toward benzene after the pre-reduction of the Re/HZSM with H_2 at 573 K and with CH_4 at 973 K proceeds with higher activities at a lower temperature, ca. 800 K, than with those on the fresh one. It is clear by the TG/DTA/mass studies that the reduction of Re oxide with hydrogen or methane results in the transformation of Re-oxide on HZSM-5 to the active phase, probably metallic Re which promotes methane activation and dehydroaromatization to C_2 hydrocarbons and benzene.

3.4. EXAFS Characterization of Re/HZSM-5 in Methane Conversion

To characterize the active phase of the Re/HZSM-5 responsible for the methane aromatization to benzene, the

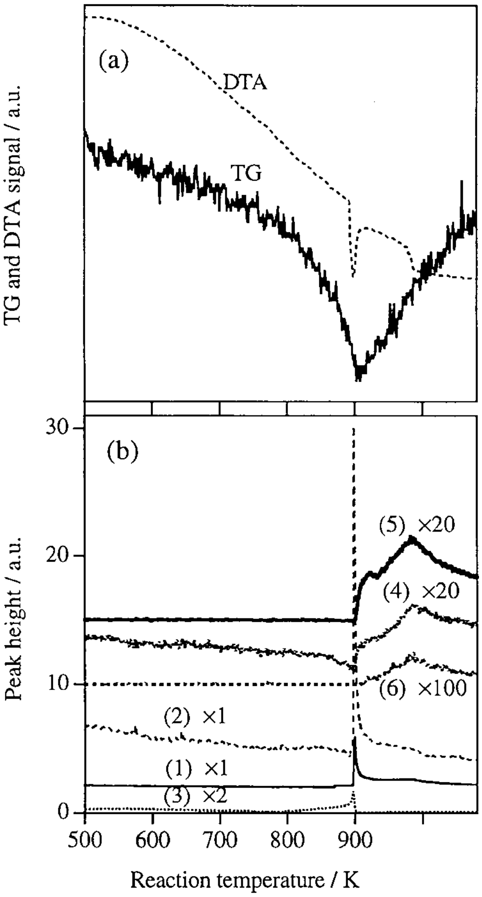

FIG. 3. TG (a), DTA (a), and mass (b) spectra of 5Re/HZSM-5 (SiO_2/Al_2O_3 ratio of 40) in the methane reaction by programmed heating (10 K/min) from 300 to 973 K and holding at 973 K for 30 min in a gas flow of CH_4 (15 ml/min) and He (150 ml/min): (**1**), (**2**), (**3**), (**4**), (**5**), and (**6**) refer to H_2, CO, CO_2, ethene, benzene, and naphthalene, respectively.

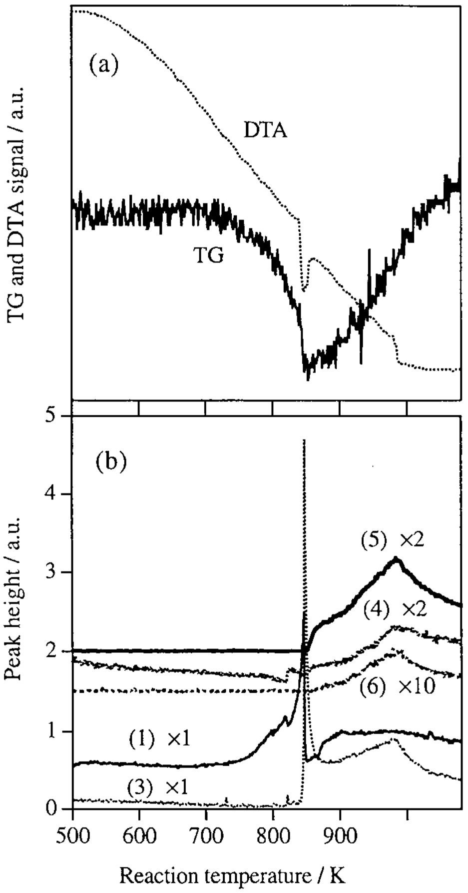

FIG. 4. TG (a), DTA (a), and mass (b) spectra under the same condition as Fig. 3 except for the following gas flows: CH_4 (15 ml/min), CO (1.8 ml/min), and He (150 ml/min).

Re L_{III}-edge EXAFS studies were conducted using the 10B beam-line at the Photon Factory of National Laboratory for High Energy Physics (KEK-PF). Figure 5 represents the Fourier transform functions of Re L_{III}-edge EXAFS spectra of 10 wt% loading Re/HZSM-5 calcined at 773 K for 4 h (**2**), pre-reduced with hydrogen at 573 K for 0.5 h (6), and reacted with methane at 973 K for 0.5 (**5**) and 24 h (**6**), respectively. The EXAFS spectra of Re powder and NH_4ReO_4 crystal were measured as references (Fig. 5, (**3**) and (**1**)). The FT spectrum in Fig. 5, (**2**) and (**6**), for the Re/HZSM-5 sample after the calcination with air at 773 K and reduction with hydrogen at 573 K was identical to that of NH_4ReO_4 (Fig. 5 (**1**)) and of Re powder (Fig. 5 (**3**)), respectively.

The two dominant peaks on each spectrum represent the Re–Re distance in Re powder (2.74 Å) and the Re–O distance in NH_4ReO_4 (1.71 Å) as the reference samples, respectively. After the calcination of the 10 wt% Re loading sample, $(NH_4)_2ReO_4$/HZSM-5, at 773 K prior to the methane reaction, the Re L_{III}-edge Fourier transform functions showed that the calcined sample (Fig. 5 (**2**)) consists of the intense peak at 1.38 Å possibly due to the Re–O bond of Re oxide species similar to the reference NH_4ReO_4. The FT function of the sample reduced at 573 K for 0.5 h (Fig. 5 (**6**)) is identical with those for the Re powder reference (Fig. 5 (**3**)) in every detail except for a minor peak at 1.42 Å, which is attributable to the Re–O bond. The structural information abstracted from the curve-fitting of the FT function for the samples of Re/HZSM-5 after reduction with H_2 (1 atm) at 573 K for 0.5 h and after the exposure to methane (3 atm) for 0.5, 4, and 24 h is listed in Table 2. After the reduction with hydrogen, the Re oxide species is converted to Re particles (Re–Re; $R = 2.74$ Å, $CN = 4.0$) in comparison with those of Re powder (Re–Re; $R = 2.74$ Å, $CN = 12$). The FT function spectra of the reduced Re/HZSM-5 after the reaction with methane at 973 K are identical each other (Fig. 5, (**4**) and (**5**)). The EXAFS parameters of the sample after the methane reaction at 973 K retained a major contribution of Re–Re ($R = 2.74$ Å, $CN = 4.9$–6.4) as indicated in Table 2. These results imply that the Re oxide species

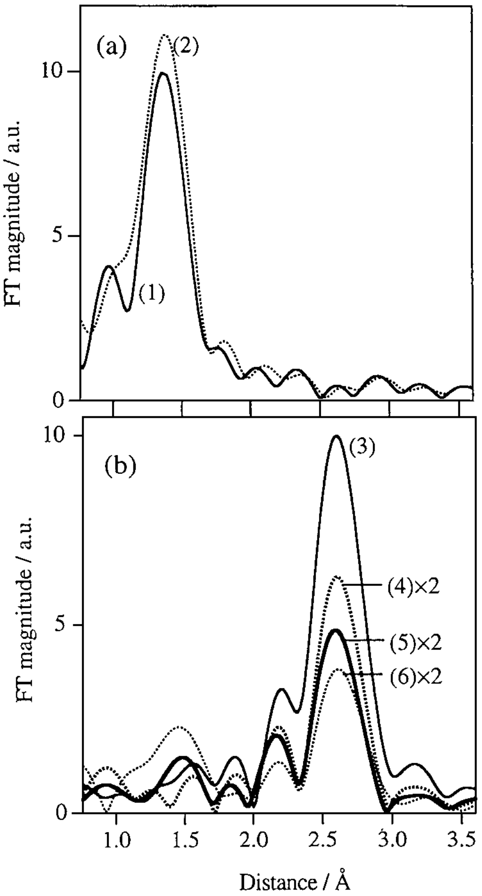

FIG. 5. Re L_{III}-edge Fourier transformed spectra of (**1**) NH_4ReO_4 crystal, (**2**) 10% Re/HZSM-5 calcined at 773 K for 4 h, (**3**) Re powder as a reference, (**4**) sample 2 treated with methane at 973 K for 24 h, (**5**) 5Re/HZSM-5 treated with methane at 973 K for 30 min, and (**6**) 5Re/HZSM-5 reduced at 573 K for 30 min.

TABLE 2

EXAFS Parameters for Re–Re Bonding Derived from R-Sphere Fitting of Re L_{III}-Edge FT Curves of Re Powder and 5% Re/HZSM-5 Treated at Various Conditions[a]

		R/Å	N	ΔE/eV	σ	r/%
Re-powder		2.74	12			
5% Re/HSM-5	in H_2 at 573 K for 1 h	2.750	4.00	−0.17	0.073	13
	in CH_4 at 973 K for 0.5 h	2.742	4.98	−3.73	0.073	17
	in CH_4 at 973 K for 4 h	2.745	4.93	−3.17	0.073	15
	in CH_4 at 973 K for 24 h	2.747	6.38	−0.72	0.074	14

[a] See method in Experimental Procedures. R, N, ΔE, σ, and r are the Re–Re interatomic distance, the coordination number, the shift of threshold energy, the Debye–Waller-like factor, and the reliability factor, respectively.

dispersed in HZSM-5 is reduced with hydrogen or methane to highly dispersed metallic Re, which is responsible for the methane aromatization toward C_2 hydrocarbons and benzene on Re/HZSM-5. By contrast, the relatively stable Mo carbide phase of Mo_2C was observed by XPS and EXAFS and, thus, it has been proposed to be active for methane activation and dehydroaromatization on Mo/HZSM-5 (4–8, 11–20).

3.5. Promotion of Dehydrocondensation of Methane by Adding CO and CO_2

As stated, methane conversion and benzene formation rate on the Re/HZSM-5 were decreased greatly using pure CH_4 as the feed gas at 1023 K, when the methane space velocity was higher than 3500 ml/g cat/h as shown in Figs. 2a and 2b. Adding CO to methane feed exerts a promoting effect on the catalytic performances of Re/HZSM-5 for the dehydroaromatization of methane to enhance the catalyst stability and the rate of benzene formation (Fig. 6). At the prolonged reaction time, the effect of CO addition to the rate of benzene formation became apparent such as 0.4 and 2.2 μmol/g cat/s for 0 and 8.6% CO in the methane feed, respectively, at 5 h of time on stream, although the initial rates of benzene formation were not different. The results imply that the active oxygen species derived from CO reacts with the surface carbon, which otherwise forms inactive coke as reactions (2) and (3) in Scheme 1. The benzene formation rate in the methane reaction was also affected by the CO concentration in the feed gas and measured under 1440 ml/g cat/h of methane space velocity where the activity was stable (Fig. 7). By varying the CO concentration from 8.6 to 22.2% in the feed gas, the rates of benzene formation more than doubled the rate in pure methane (Fig. 7b). In fact, the rate of total hydrocarbon formation exceeded the rate of methane conversion at 12 and 22% CO in the feed, suggesting that a part of CO participates in forming hydrocarbons as in reaction (1) of Scheme 1. However, the rate of benzene formation on Mo/HZSM-5 did not increase with addition of CO in methane feed.

As shown in Fig. 6, the stability of the catalyst was significantly improved by adding a few percent of CO_2 into the feed gas on Re/HZSM-5 (Fig. 8). The addition of 1% CO_2 yielded a higher methane conversion and rate of benzene formation. Even at 5000 ml/g cat/h of methane space velocity, the rate of benzene formation was kept constant by adding 2% CO_2 in the feed for more than 6 h. Furthermore, the coke formation was substantially suppressed in

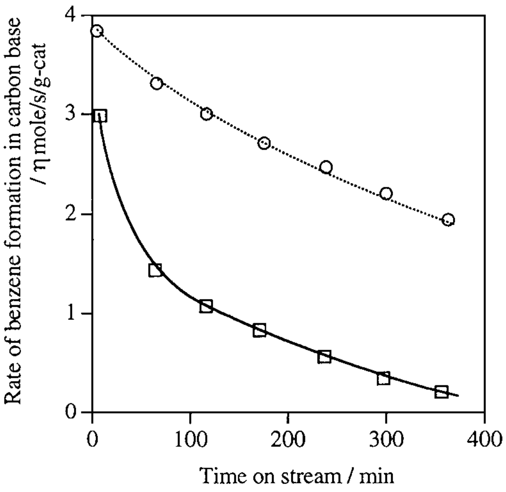

FIG. 6. Rate of benzene formation in the methane reaction at 1023 K, 3 atm, and 5000 ml/g cat/h of methane space velocity in a methane flow (□) and in methane + 8.6% CO flow (○).

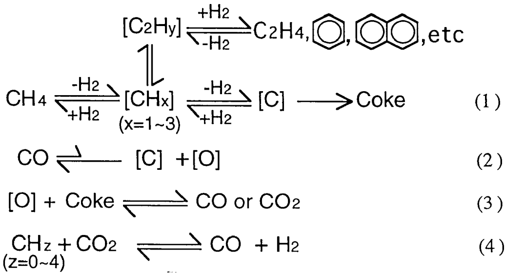

SCHEME 1

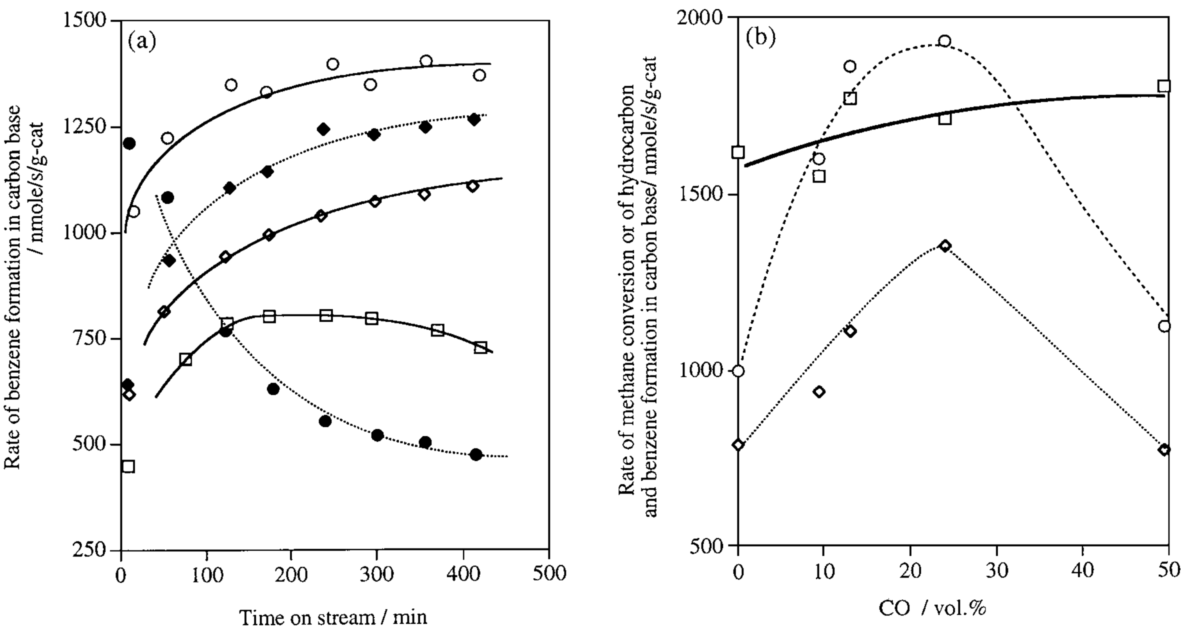

FIG. 7. Catalytic performance of 5Re/HZSM-5 for methane aromatization with the addition of CO in the methane feed at 1023 K, 3 atm, and 1440 ml/g cat/h of methane space velocity. (a) Rate of benzene formation vs time on stream by varying CO %, such as □, ◇, ◆, ○, ● for 0, 8.6, 11.9, 22.2, 46.8 in the feed, respectively. (b) Rate of methane conversion (□), hydrocarbon formation (○), and benzene formation (◇) vs CO % in the feed.

the methane dehydroaromatization at 3 atm and 1023 K on Re/HZSM-5 by addition of 1.8–3.0% CO_2 to the methane feed. It is demonstrated that CO_2 is converted with CH_x ($x = 0$–4) to produce double the amount of CO under the reaction condition by the reaction (4) in Scheme 1. The CO formed may exert a similar promotion of the dehydroaromatization of methane and improvement of the catalytic stability. However, addition of excess CO_2 (more than 4%) results in the marked decrease of rates of benzene formation for the methane aromatization on the Re/HZSM-5 catalysts.

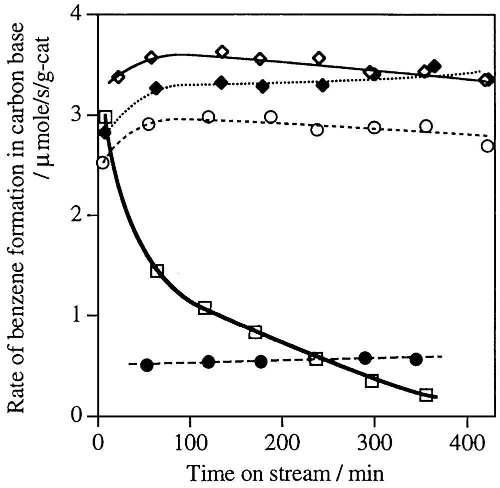

FIG. 8. Catalytic performance of 5Re/HZSM-5 for methane aromatization with the addition of □, ◇, ◆, ○, ● for 0, 1, 2, 3, 8.6% CO_2, respectively, in the feed at 1023 K, 3 atm, and 5000 ml/g cat/h of methane space velocity.

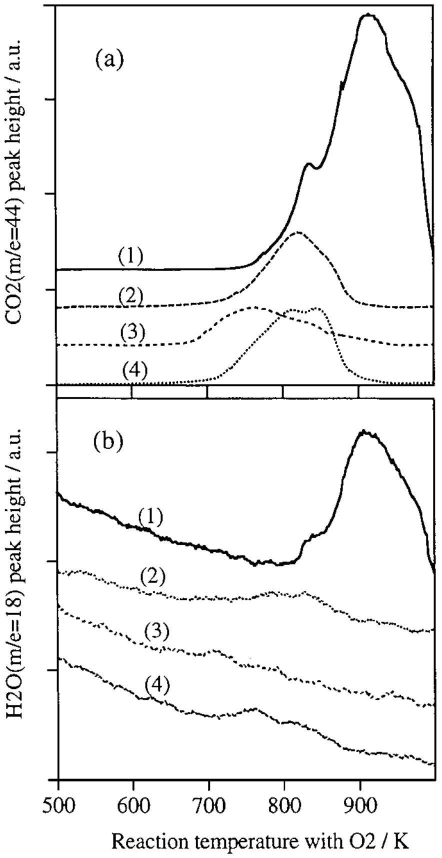

FIG. 9. TPO pattterns as CO_2 (a) and H_2O (b) formation by flowing O_2/He (20/150 = ml/min) on the 5Re/HZSM-5 catalysts after the reaction with (1) CH_4, (2) $CH_4 + 1\%$ CO_2, (3) $CH_4 + 8\%$ CO_2, and (4) $CH_4 + 11\%$ CO at 1023 K, 3 atm, and methane space velocity = 1440 ml/g cat/h.

As shown in Fig. 9, it was demonstrated by the TPO experiments (ramping temperature rate: 10 K/min, O_2/He flow (20/150 ml/min)) that the amount of coke deposition on the catalyst surface was greatly reduced by adding various amounts of CO or CO_2 to the methane feed gas. The increase in CO concentration from 1.7 to 12.0% in methane flow resulted in a marked suppression of the total coke formation on the catalyst surface, particularly the irreversible or inert coke which was oxidized to CO_2 at the higher temperature above 773 K in the TPO experiment. The increase in CO_2 partial pressure (1.4–4.0%) in methane feed decreased effectively the coke formation on the catalyst to a much lower level, compared with that of CO. This may be related to its higher activity in the reaction with surface carbon to form CO ($CO_2 + C \rightarrow 2CO$, reaction 4 in Scheme 1, $z = 0$). This promotional role of CO/CO_2 addition to methane feed is analogous to that occurring in the dehydrocondensation of methane toward benzene on Mo/HZSM-5, owing to the effective removal of surface carbon to stabilize the catalytic performance under the prevailing conditions (14–17).

4. CONCLUSION

(1) Catalytic dehydroaromatization of methane proceeds at the temperatures of 873–1023 K under 3 atm of methane on 5Re/HZSM-5 to yield C_2 hydrocarbons and aromatic products such as benzene and naphthalene with similar activity and selectivities, compared with that on Mo/HZSM-5.

(2) Adding a few percent of CO/CO_2 to methane feed gas exerts a significant promoting effect on the catalytic performances of Re/HZSM-5 for the aromatization reaction to enhance the benzene formation and catalyst stability, owing to the effective suppression of coke formation on the catalysts.

(3) TG/DTA/mass and EXAFS studies revealed that the Re oxide species dispersed in the calcined HZSM-5 is reduced with hydrogen at 573 K or methane at 895 K to metallic Re, which is responsible for methane activation and dehydroaromatization toward C_2 hydrocarbons and benzene on Re/HZSM-5.

ACKNOWLEDGMENT

This work was supported by the Proposal-Based New Industry Creative Type Technology R&D Promotion Program from the New Energy and Industrial Technology Development Organization (NEDO) of Japan.

REFERENCES

1. Wang, L., Tao, L., Xie, M., Xu, G., Huang, J., and Xu, Y., *Catal. Lett.* **21**, 35 (1993).
2. Xu, Y., Liu, S., Wang, L., Xie, M., and Guo, X., *Catal. Lett.* **30**, 135 (1995).
3. Xu, Y., Liu, W., Wong, S., Wang, L., and Guo, X., *Catal. Lett.* **40**, 207 (1996).
4. Solymosi, F., Erdöhelyi, A., and Szöke, A., *Catal. Lett.* **32**, 43 (1995).
5. Solymosi, F., Szöke, A., and Cserényi, J., *Catal. Lett.* **39**, 157 (1996).
6. Szöke, A., and Solymosi, F., *Appl. Catal. A: General* **142**, 361 (1996).
7. Solymosi, F., Cserényi, J., Szöke, A., Bánsagi, T., and Oszkó, A., *J. Catal.* **165**, 156 (1997).
8. Wong, S.-T., Xu, Y., Wang, L., Liu, S., Li, G., Xie, M., and Guo, X., *Catal. Lett.* **38**, 39 (1996).
9. Shu, Y., Xu, Y., Liu, S., Wang, L., and Guo, X., *J. Catal.* **170**, 11 (1997).
10. Liu, W., Xu, Y., Wong, S.-T., Qiu, J., and Yang, N., *J. Mol. Catal. A: Chem.* **120**, 257 (1997).
11. Liu, S., Dong, Q., Ohnishi, R., and Ichikawa, M., *J. Chem. Soc., Chem. Commun.* 1455 (1997).
12. Wang, D., Lunsford, J. H., and Rosynek, M. P., *J. Catal.* **169**, 347 (1997).
13. Wang, D., Lunsford, J. H., and Rosynek, M. P., *Topics Catal.* **3**, 289 (1996).
14. Liu, S., Wang, L., Ohnishi, R., and Ichikawa, M., *Chem. Commun.* 1217 (1998).
15. Liu, S., Wang, L., Dong, Q., Ohnishi R., and Ichikawa, M., *Stud. Surf. Sci. Catal.* **119**, 241 (1998).
16. Liu, S., Wang, L., Ohnishi R., and Ichikawa, M., *J. Catal.* **181**, 175 (1999).
17. Ohnishi, R., Liu, S., Dong, Q., Wang, L., and Ichikawa, M., *J. Catal.* **182**, 92 (1999).
18. Weckhuysen, B. M., Wang, D., Rosynek, M. P., and Lunsford, J. H., *J. Catal.* **175**, 347 (1998).
19. Weckhuysen, B. M., Wang, D., Rosynek, M. P., and Lunsford, J. H., *J. Catal.* **175**, 338 (1998).
20. Zhang, J. Z., Long, M. A., and Howe, R. F., *Catal. Today* **44**, 293 (1999).
21. Oyama, S. T., Schlatter, J. C., Metcalfe, J. E., III, and Lambert, J. M., Jr., *Ind. Eng. Chem. Res.* 1639 (1988).
22. Borry, R. W., III, Kim, Y. H., Huffsmith, A., Reimer, J. A., and Inglesia, E., *J. Phys. Chem. B* **103**, 5787 (1999).